

Generation and recovery of strain in ^{28}Si -implanted pseudomorphic GeSi films on Si(100)

G. Bai^(a) and M.-A. Nicolet
California Institute of Technology, Pasadena, California 91125

(Received 28 October 1991; accepted for publication 29 January 1992)

Effects of ion implantation of 320 keV ^{28}Si at room temperature in pseudomorphic metastable $\text{Ge}_x\text{Si}_{1-x}$ ($x \approx 0.04, 0.09, 0.13$) layers ~ 170 nm thick grown on Si(100) wafers were characterized by x-ray double-crystal diffractometry and MeV ^4He channeling spectrometry. The damage induced by implantation produces additional compressive strain in the $\text{Ge}_x\text{Si}_{1-x}$ layers, superimposed on the intrinsic compressive strain of the heterostructures. This strain rises with the dose proportionally for doses below several times 10^{14} $^{28}\text{Si}/\text{cm}^2$. Furthermore, for a given dose, the strain increases with the Ge content in the layer. Upon thermal processing, the damage anneals out and the strain recovers to the value before implantation. Amorphized samples (doses of greater than 2×10^{15} $^{28}\text{Si}/\text{cm}^2$) regrow poorly.

INTRODUCTION

Recent interest in GeSi-base heterojunction bipolar transistors has spurred numerous studies on various properties of GeSi/Si structures, including the effect of ion implantation. The higher atomic number of Ge rather than Si results in heavier damage in the GeSi than in the Si layers, which can induce amorphous-crystalline superlattices.^{1,2} Amorphized GeSi layers on crystalline Si recrystallize epitaxially upon thermal processing.^{3,4} Defects produced in a metastable strained layer by ion implantation enhance strain relaxation.⁵ Strain modification was observed in ion-assisted deposition of GeSi films.⁶ We report here some results on the strain and damage induced by 320 keV ^{28}Si implantation into pseudomorphic GeSi layers on Si(100), and the effects of thermal annealing. The stability of ion-implanted strained layers is also discussed.

EXPERIMENTAL PROCEDURES

Pseudomorphic metastable $\text{Ge}_x\text{Si}_{1-x}$ ($x \approx 0.04, 0.09, 0.13$) layers ~ 170 nm thick were grown on Si(100) wafers at ~ 600 °C by ultrahigh-vacuum chemical vapor deposition at IBM.⁷ The samples were sent to Caltech where they were analyzed by backscattering spectrometry to determine the composition and the thickness of the films, and by x-ray rocking curves to establish the strain state of the films. The samples were degreased before being loaded into the implanter. 320 keV ^{28}Si ions were implanted into the samples at room temperature in vacuum ($\sim 10^{-7}$ Torr). The damage peaks at ~ 200 nm beneath the interface inside the Si substrate, according to TRIM88 simulation.⁸ The ^{28}Si dose, ϕ , ranges from $10^{14}/\text{cm}^2$ to $2 \times 10^{15}/\text{cm}^2$, and the flux was kept below $10^{12}/\text{cm}^2$ s. Double-crystal diffractometry and MeV ion channeling were used to analyze the strain and damage induced by implantation.

Samples were also annealed for 30 min at 300–700 °C in vacuum ($\sim 5 \times 10^{-7}$ Torr). The recovery of damage and the change of strain in the GeSi layers were monitored.

^(a)Present address: Intel Corp., 3065 Bowers Ave., SC1-03, Santa Clara, CA 95052-8126.

RESULTS AND DISCUSSION

The perpendicular and parallel strain, ϵ^\perp and ϵ^\parallel , in the GeSi/Si(100) heterostructures were extracted from Fe $K_{\alpha 1}$ x-ray (wavelength = 0.1936 nm) rocking curves of both symmetrical (400) and asymmetrical (311) diffractions. All the as-grown samples are pseudomorphic within experimental sensitivity ($\epsilon^\parallel \leq 0.01\%$), in agreement with the experimental results of Ref. 9. These samples are metastable, meaning that they are all thicker than the equilibrium critical thickness predicted by Matthews–Blakeslee’s model.¹⁰ Figure 1 shows the (400) rocking curves of the as-grown $\text{Ge}_{0.09}\text{Si}_{0.91}/\text{Si}(100)$ (solid line) and of the samples implanted to doses of 2×10^{14} $^{28}\text{Si}/\text{cm}^2$ (\bullet) and 5×10^{14} $^{28}\text{Si}/\text{cm}^2$ (\circ). The rocking curve of the as-grown sample shows clearly visible small-amplitude oscillations, indicating a high crystalline perfection of the $\text{Ge}_{0.09}\text{Si}_{0.91}$ layer. The angular width of the diffraction peak from the layer is due entirely to the finite thickness of the layer. The perpendicular strain of the as-grown sample is $\epsilon^\perp = 0.69\%$. After implantation to 2×10^{14} $^{28}\text{Si}/\text{cm}^2$, the diffraction peak from the $\text{Ge}_{0.09}\text{Si}_{0.91}$ layer shifts farther away from the substrate Si peak, meaning that the layer develops an additional positive strain (see \bullet in Fig. 1). The peak intensity decreases, while the angular width remains about the same. These facts suggest that defects are produced in the layer, that the layer still diffracts x-ray coherently, and that the defects are laterally uniformly distributed in the layer and induce uniform lattice expansion. The perpendicular strain of the implanted sample is $\epsilon^\perp = 0.97\%$, while the parallel strain remains zero. The sample is thus still pseudomorphic and becomes more metastable than it was before. The additional perpendicular strain induced by the implantation damage, $\Delta\epsilon^\perp$, is 0.28%. One can also see the diffraction peak (at $\sim -0.05^\circ$ near the Si reference peak) from the damaged substrate Si (\bullet in Fig. 1). The strain induced ($\sim 0.06\%$) is about the same as that in the implanted bulk Si samples,¹¹ suggesting that the $\text{Ge}_{0.09}\text{Si}_{0.91}$ overlayer has no influence on the implantation damage in the Si substrate. As the dose rises to 5×10^{14} $^{28}\text{Si}/\text{cm}^2$, the diffraction peak from the GeSi layer is buried in the background and

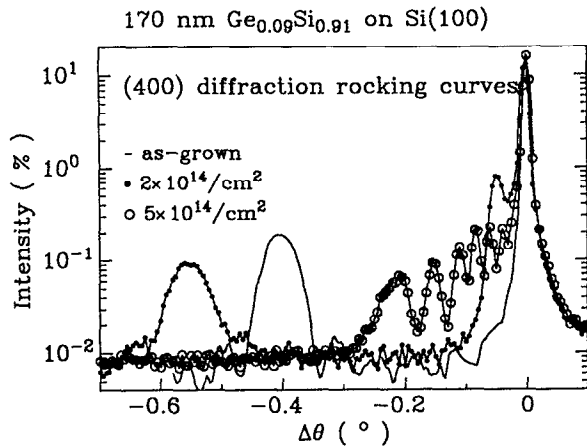


FIG. 1. Fe K_{α} x-ray rocking curves for symmetrical (400) diffractions of $\text{Ge}_{0.09}\text{Si}_{0.91}/\text{Si}(100)$ samples ($\theta_B = 45.5^\circ$): as-grown (solid line) and implanted at room temperature with 320 keV ^{28}Si to 2×10^{14} $^{28}\text{Si}/\text{cm}^2$ (●), 5×10^{14} $^{28}\text{Si}/\text{cm}^2$ (○).

becomes undetectable, while that from the damaged Si substrate is still measurable (○ in Fig. 1). These findings indicate that the $\text{Ge}_{0.09}\text{Si}_{0.91}$ layer is more severely damaged than the Si substrate. In other words, the $\text{Ge}_{0.09}\text{Si}_{0.91}$ alloy is more susceptible to radiation damage than Si is, in agreement with others' results.^{1,2} Although the $\text{Ge}_{0.09}\text{Si}_{0.91}$ layer doesn't produce a measurable x-ray diffraction peak, it is not yet amorphized by this dose of 5×10^{14} $^{28}\text{Si}/\text{cm}^2$, as the [100] axial channeling spectrum of 2 MeV ^4He indicates (minimum yield $\sim 80\%$). As the dose increases further to 2×10^{15} $^{28}\text{Si}/\text{cm}^2$, the rocking curve from the sample becomes featureless (not shown) because both the layer and the substrate are amorphized (minimum yield $\sim 100\%$).^{11,12}

X-ray rocking curve measurements of other implanted samples with different Ge composition give results similar to those described above. First, the strain in the damaged substrate Si is that expected in the implanted bulk Si.¹¹ Second, the implantation damage induces additional strain in the GeSi layer besides the intrinsic strain of the heterostructure. The layers remain pseudomorphic. At low damage level ($\phi < 2 \times 10^{14}$ $^{28}\text{Si}/\text{cm}^2$) where the diffraction peak from the GeSi layers is measurable, the additional strain induced by damage, $\Delta\epsilon^\perp$, increases with the implantation dose (Fig. 2). We know that the strain increases linearly with the Si dose at low damage levels in implanted bulk Si¹¹ and Ge¹³ crystals. The limited data in Fig. 2 and the analogy with Si and Ge lead us to propose that for any Ge composition, $\Delta\epsilon^\perp$ is proportional to the dose at low damage levels. For a given dose, the induced strain in the GeSi alloy increases linearly with the Ge composition (Fig. 2). The dashed line is that obtained by interpolation between the corresponding strain of implanted Si and Ge. For that interpolation, the strain in implanted Si can be found directly from the measurements.¹¹ The strain for implanted Ge was computed by multiplying the slope of strain versus dose by the corresponding dose ($1.2 \times$ or 2×10^{14} $^{28}\text{Si}/\text{cm}^2$), because this strain cannot be realized physically

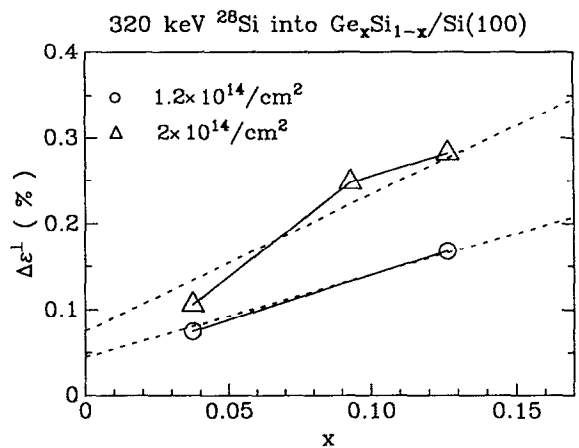


FIG. 2. The strain induced by 320 keV ^{28}Si implantation into pseudomorphic GeSi layers vs the Ge composition. The dashed lines are the strains predicted from a linear interpolation model of Eq. (1).

since the Ge is amorphized beyond $\sim 7 \times 10^{13}$ $^{28}\text{Si}/\text{cm}^2$. Figure 2 shows that the interpolation approximates the data well. This result suggests that the slope, $S_{\text{Ge}_x\text{Si}_{1-x}}$, of the implantation-induced strain $\Delta\epsilon^\perp$ versus the dose ϕ for $\text{Ge}_x\text{Si}_{1-x}$ alloy at low damage level (linear damage regime), may be predicted from those of Ge and Si, S_{Ge} and S_{Si} according to

$$S_{\text{Ge}_x\text{Si}_{1-x}} = xS_{\text{Ge}} + (1-x)S_{\text{Si}}. \quad (1)$$

Additional experiments are desirable to test this relationship over the entire Ge compositions ($0 \leq x \leq 1$).

To investigate the stability of these implanted layers upon thermal processing, we annealed the samples at 300–700 °C in vacuum for 30 min and monitored the change of strain at room temperature after the heat treatment. First, we noticed that the annealing characteristics of the damaged Si substrate are similar to those of implanted bulk Si samples.¹¹ The annealing behavior of the $\text{Ge}_{0.09}\text{Si}_{0.91}$ layers can be categorized into three types according to the initial damage level. For the lightly damaged samples ($\phi \leq 2 \times 10^{14}$ $^{28}\text{Si}/\text{cm}^2$), the annealing shifts the $\text{Ge}_{0.09}\text{Si}_{0.91}$ diffraction peak towards the main peak, and the peak intensity increases. The peak width remains the same. The rocking curve eventually reverses back to that of the as-grown sample after 700 °C. For the heavily damaged samples ($\phi = 5 \times 10^{14}$ $^{28}\text{Si}/\text{cm}^2$, ○ in Fig. 3) where the peak from the implanted $\text{Ge}_{0.09}\text{Si}_{0.91}$ layer becomes undetectable, that peak remains undetectable after 300 °C (filled inverse triangle in Fig. 3), but becomes measurable after 400 °C annealing (●), and the samples completely recover after 700 °C (solid line in Fig. 3). Figure 4 plots the perpendicular strain of the three samples studied here as a function of temperature for 30 min annealing. The filled symbols represent the as-grown samples. Two conclusions are evident: (a) the major annealing stage occurs below 300 °C, and (b) the strain and damage induced by the implantation heals out completely upon heating at 700 °C. Furthermore, no relaxation of the intrinsic strain is ob-

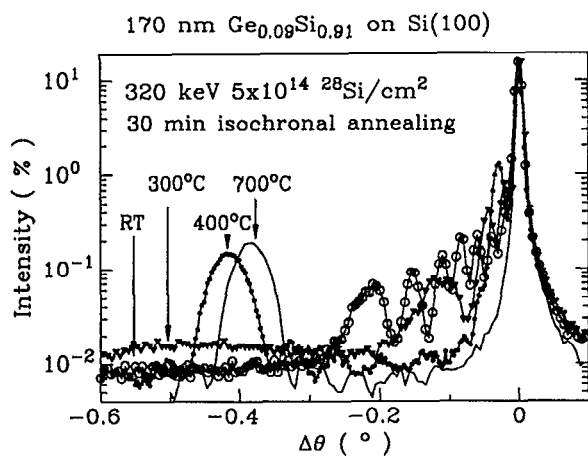


FIG. 3. (400) x-ray rocking curves of a pseudomorphic $\text{Ge}_{0.09}\text{Si}_{0.91}/\text{Si}(100)$ implanted at room temperature (RT, \circ) by 320 keV $5 \times 10^{14} \text{ }^{28}\text{Si}/\text{cm}^2$ and annealed for 30 min at 300 °C (∇), 400 °C (\bullet), and 700 °C (solid line). The spectrum of the sample annealed at 700 °C (solid line) is indistinguishable from that of the as-grown sample (solid line of Fig. 1).

served for any sample after 700 °C annealing, meaning that the presence of defects does not significantly enhance the relaxation of the metastable strain. Hull *et al.*⁵ did observe some enhancement of strain relaxation in implanted GeSi/Si structures by transmission electron microscopy. These authors suggested that the defects promote the nucleation of dislocations, but impede their propagation. The x-ray rocking curve technique is not sensitive enough to explore that regime of initial dislocation nucleations because the dislocation density is below the x-ray detection limit which lies at a total length of misfit dislocations per unit area of about $10^4/\text{cm}$.

The third type of annealing behavior is found for samples irradiated by $2 \times 10^{15} \text{ }^{28}\text{Si}/\text{cm}^2$ in which both the

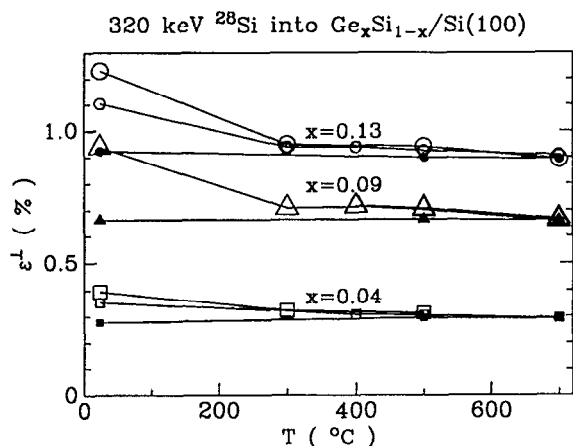


FIG. 4. The strain in the $\text{Ge}_x\text{Si}_{1-x}$ layer vs the annealing temperature. The square, triangle, and circle are for the samples with $x = 0.04, 0.09, 0.13$, respectively. The filled symbols represent the unimplanted samples. The small (big) open symbols represent the samples implanted by 320 keV $1.2 \times (2 \times) 10^{14} \text{ }^{28}\text{Si}/\text{cm}^2$.

$\text{Ge}_x\text{Si}_{1-x}$ layer and the Si substrate were amorphized. We used x-ray diffraction and MeV ion channeling to study the solid-phase epitaxial regrowth of these three samples with composition $x \approx 0.04, 0.09, 0.13$. The regrown layers have larger channeling yields, and much weaker and broader x-ray diffraction peaks than the as-grown layers, indicating the presence of extended defects in the layers. To maintain the crystalline perfection of epitaxial GeSi layers, amorphization transformation of the GeSi layers should thus be avoided.

CONCLUSION

In summary, we find that the damage produced by ^{28}Si implantation in pseudomorphic GeSi layers on Si(100) induces additional compressive strain in the layers. At a low damage level, the induced strain increases linearly with the dose. The slope of the induced strain versus the dose rises linearly with the Ge composition, and can be predicted by interpolation of the slopes for bulk Ge and Si crystals. Thermal annealing removes damage and eliminates the implantation-induced strain. Damaged, but not amorphized, samples fully recover after 700 °C annealing for 30 min; amorphized samples recover only partially. In Si, implanted dopants are activated most effectively when Si is fully amorphized prior to thermal annealing. For epitaxial GeSi layers on Si, that procedure would appear problematic in the light of the present results.

ACKNOWLEDGMENTS

We would like to thank Dr. Akbar at IBM for providing the as-grown GeSi/Si(100) samples. This paper is based upon the work supported in part by the Semiconductor Research Corporation under contract No. 91-SJ-100.

- ¹D. J. Eaglesham, J. M. Poate, D. C. Jacobson, M. Cerullo, L. N. Pfeiffer, and K. West, *Appl. Phys. Lett.* **58**, 523 (1991).
- ²M. Vos, C. Wu, I. V. Mitchell, T. E. Jackman, J.-M. Baribeau, and J. McCaffrey, *Appl. Phys. Lett.* **58**, 951 (1991).
- ³B. T. Chilton, B. J. Robinson, D. A. Thompson, T. E. Jackman, and J.-M. Baribeau, *Appl. Phys. Lett.* **54**, 42 (1989).
- ⁴S. Mantl, B. Holländer, W. Jäger, B. Kabins, H. J. Jorke, and E. Kasper, *Nucl. Instrum. Methods B* **39**, 405 (1989).
- ⁵R. Hull, J. C. Bean, J. M. Bonar, G. S. Higashi, K. T. Short, H. Temkin, and A. E. White, *Appl. Phys. Lett.* **56**, 2445 (1990).
- ⁶C. J. Tsai, H. A. Atwater, and T. Vreeland, *Appl. Phys. Lett.* **57**, 2305 (1990).
- ⁷B. S. Meyerson, *Appl. Phys. Lett.* **48**, 791 (1986).
- ⁸J. P. Biersack and L. G. Haggmark, *Nucl. Instrum. Methods* **174**, 257 (1980).
- ⁹J. C. Bean, L. C. Feldman, A. T. Fiory, S. Nakahara, and I. K. Robinson, *J. Vac. Sci. Technol. A* **2**, 436 (1984).
- ¹⁰J. W. Matthews and A. E. Blakeslee, *J. Cryst. Growth* **27**, 118 (1974).
- ¹¹G. Bai and M.-A. Nicolet, *J. Appl. Phys.* **70**, 649 (1991).
- ¹²V. S. Speriosu, B. M. Paine, M.-A. Nicolet, and H. L. Glass, *Appl. Phys. Lett.* **40**, 604 (1982).
- ¹³G. Bai and M.-A. Nicolet (unpublished data).